Soft Matter

Accepted Manuscript

ROYAL SOCIETY OF CHEMISTRY

www.rsc.org/softmatter

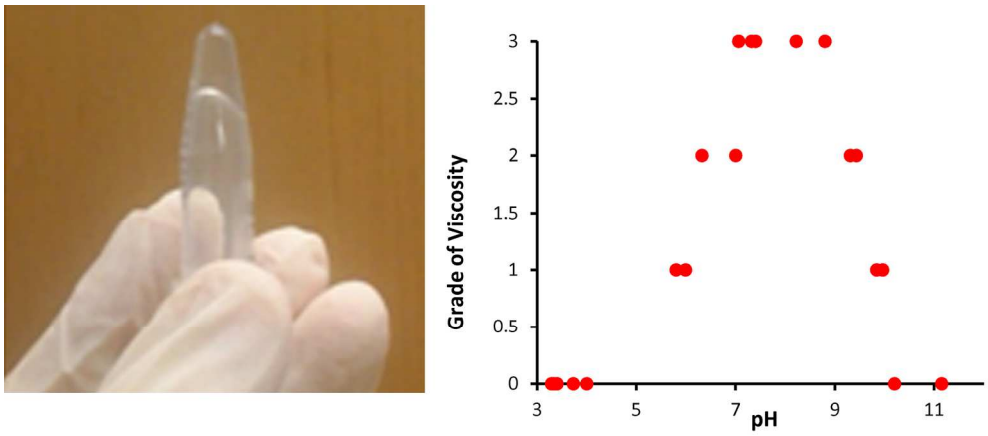

The GSFSIQYTYHV peptide forms a clear hydrogel around neutral pH.

The 11-residue peptide GSFSIQYTYHV from human semenogelin I forms a hydrogel with optimal stability at pH 7-9.

Journal Name

RSCPublishing

ARTICLE

A Peptide from Human Semenogelin I Self-Assembles into a pH-Responsive Hydrogel

B. Frohm,[a] J. E. DeNizio,[b,c] D. S. M. Lee,[b,d] L. Gentile,[e] U. Olsson,[e] J. Malm,[f] K. S. Åkerfeldt,[b*] and S. Linse[a*]

Cite this: DOI: 10.1039/x0xx00000x

Received 00th January 2012,
Accepted 00th January 2012

DOI: 10.1039/x0xx00000x

www.rsc.org/

The peptide GSFSIQYTYHV derived from human semenogelin I forms a transparent hydrogel through spontaneous self-assembly in water at neutral pH. Linear rheology measurements demonstrate that the gel shows a dominating elastic response over a large frequency interval. CD, fluorescence and FTIR spectroscopy and *cryo*-TEM studies imply long fibrillar aggregates of extended β-sheet. Dynamic light scattering data indicate that the fibril lengths are of the order of micrometers. Time-dependent thioflavin T fluorescence shows that fibril formation by GSFSIQYTYHV is a nucleated reaction. The peptide may serve as basis for development of smart biomaterials of low immunogenicity suitable for biomedical applications, including drug delivery and wound healing.

Introduction

Hydrogels constitute a broad and diverse class of water-soluble polymers with capacity to absorb and hold large amounts of water within a porous, swelled structure.[1] This characteristic confers many unique properties to hydrogels making them particularly well suited for biomedical applications.[2] These polymers are derived from a diverse range of compounds of natural[3] or synthetic[4] origin. A gel may arise through intermolecular interactions between self-assembled aggregates. In these gels, the networks are typically held together by molecular entanglements governed by physicochemical parameters such as pH, ionic strength and temperature, A gel may also consist of covalent networks produced through chemical cross-linking, in which the cross-linking density and primary structure of the chains control the overall properties of the gel. Rheologically, a gel is typically characterized by a storage modulus G' that is significantly greater than the loss modulus G'' over a wide range of frequencies. [1a,5]

Among a range of different possible scaffolds, peptides have emerged as particularly promising candidates for hydrogel based biomedical applications.[6] With their broad range of physical properties and chemical adaptability, they can be adopted for a range of applications within the field of biomedicine where swelling properties, viscoelasticity and stability towards degradation are key factors that determine the best application, such as whether it is most suitable as an injectable or an implantable material.[7] Peptides, with their unique set of chiral amino acid building blocks, may self-assemble in a reaction governed by the hydrophobic effect, hydrogen bonding, van der Waals' and electrostatic interactions. In contrast to many other polymeric hydrogels, peptide-based scaffolds may take on highly organised structures. Such well-defined assemblies give peptide-based gels unique properties that can be tuned in a controlled manner. Peptide hydrogels can be structurally characterized by a variety of spectroscopic methods and their properties directly related to structure and ultimately, to the amino acid sequence.[8] The types of available amino acid side chains increases the repertoire of additional manipulations that can be done to the system. Response to a change in pH, temperature or ionic strength provides means to incorporate biocompatible on-off switches.[9]

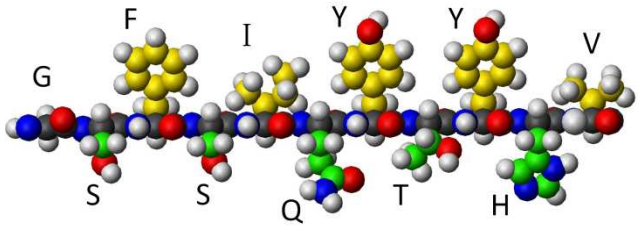

Figure 1. **SgI:38-48 sequence.** The sequence H_2N-GSFSIQYTYHV-COOH is illustrated with carbon atoms located in hydrophobic and aromatic side-chains in yellow and carbon atoms in hydrophilic side chains in green. Otherwise a conventional colour scheme is used with red, blue and white for oxygen, nitrogen and hydrogen, respectively.

Most reported peptide-derived hydrogels are designed sequences that have been manipulated to fold into a helical or a β-sheet secondary

structural unit within a self-assembled aggregate. In many designs a binary sequence of hydrophobic and hydrophilic residues are introduced to favour the formation of a particular secondary structure. Sequences have also been inspired by the amino acid composition found in peptides forming amyloid fibrils[10] and in the assembly of nanotubes and other types of nanostructures. [11,12]

Hydrogels as biomaterials have a wide range of applications, including tissue regeneration, wound healing and drug delivery.[13] Biomedical applications of hydrogels require low immunogenicity and low cytotoxicity and therefore, peptides of natural origin are particularly desirable in this regard as they are likely to elicit a low immune response.

Here, we report the discovery of a hydrogel-forming peptide of human origin. The peptide, GSFSIQYTYHV, is derived from human semenogelin I, SgI, a protein expressed in seminal vesicles, kidney, trachea, lung tissue and retina.[14] The 11-residue peptide, with a sequence of alternating polar and non-polar residues, corresponds to residues 38-48 in SgI (Figure 1). Interestingly, the prostate-specific antigen (PSA), the major protease in seminal plasma, cleaves SgI at several specific sites. One cleavage site, at residue 44, is located in the center of the gel forming peptide, indicating that the 38-48 region is important for gel formation and liquefaction in the natural processing of the protein (for more details, see SI, Figure SI-1 and SI-2). The peptide and its gel formation properties were characterized using Fourier transform infrared (FTIR) circular dichroism (CD) and fluorescence spectroscopy, rheology measurements, *cryo*-transmission electron microscopy (*cryo*-TEM) and cell viability studies. In our discussion we will adhere to terminology used in the current literature and refer to the highly viscous state as a gel (hydrogel), although there is no evidence for long-lived crosslinks or associations in the network, as found for example in gelatine and related systems. In fact, it is possible to interpret the present findings in terms of a viscoelastic solution of long overlapping rigid peptide fibrils.

Results and discussion

Hydrogel formation

Gel formation of the SgI:38-48 peptide was studied as a function of pH. Samples of lyophylised peptide (4 mM = 5 mg/mL) were dissolved in water at 22 °C. This results in clear samples with water-like viscosity and acidic pH (around 3) due to remaining TFA traces from the reversed phase HPLC purification. In an initial study, dilute NaOH was titrated into the peptide samples, which were examined by visual inspection (Figure 2a). Up to pH 4, water-like viscosity was seen. A progressive solidification was observed upon neutralization and a highly viscous gel was present between pH 7 and 9At even higher pH, around pH 10 and up, the gel began to "melt" and the samples liquefy. By eye, the peptide was thereby observed to form a hydrogel in pure water between pH 6 and 10, with the highest viscosity between pH 7 and 9. In this range the NaOH added to 4 mM peptide results in ca. 8 mM Na^+, providing relatively low screening of electrostatic interactions. We note that the strongest gel forms around the isoelectric point of 7.8. The gel formed is relatively fragile and readily breaks upon mechanical manipulation.

The peptide self-assembly was also evaluated using dynamic light scattering (DLS). This method allowed peptide samples to be investigated at a 10-fold lower concentration, at 0.4 mM (0.5 mg/mL). While the sample-to-sample reproducibility of the auto-

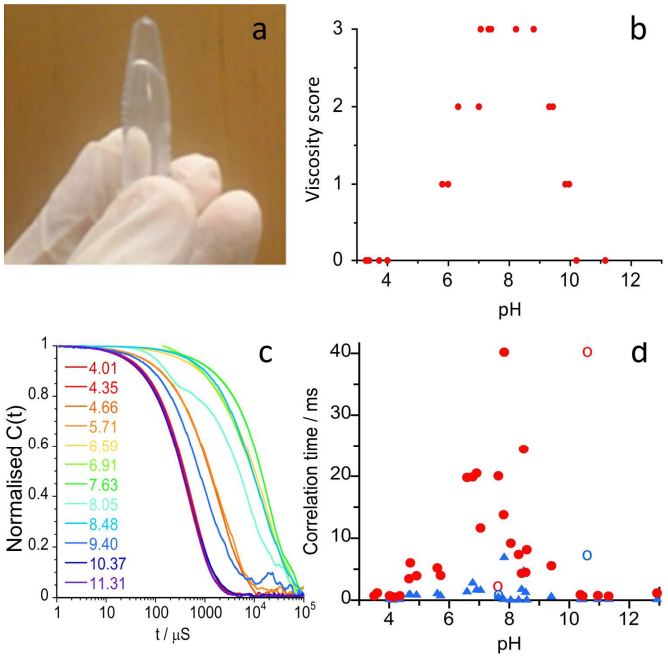

Figure 2. **pH-dependent hydrogel formation.** All samples were studied in water at 25 °C. **a)** Photograph of a tube with the clear hydrogel formed by 4 mM SgI:38-48 at pH 9.0. **b)** Viscosity score as a function of pH, graded by slow rotation of the tube and ocular inspection as water-like (0), slow-flowing (1), partly sticking to tube wall (2) and highly viscous (3) **c-d)** DLS data for 0.4 mM SgI:38-48. **c)** Normalized auto-correlation function, $C(t)$, for some selected samples within the studied pH range. **d)** Correlation times obtained from fitting a double exponential decay to $C(t)$ at each pH value. The two correlation times are shown as blue triangles (fast mode, τ_f) and filled red circles (slow mode, τ_s). Two outliers are shown as open blue and red circles.

correlation function, $C(t)$, was low in terms of signal intensity, its shape as a function of pH was found to be reproducible. Therefore, C(t) observed for each sample was normalized to between 1.0 and 0.0 with examples of data shown in Figure 2c. Below pH 5 and above pH 10, C(t) decays rapidly as expected for a highly mobile system. At intermediate pH values, C(t) decays more slowly reporting on a less mobile system. The most slowly decaying $C(t)$, is found between 7 and 9, which we interpret as the most stable gel being formed in this pH range. The autocorrelation function at low and high pH showed an essentially single exponential decay. At intermediate pH, where the gel is formed, a clear deviation from a single exponential decay was observed. Here, $C(t)$ is well described by the sum of two exponentials. For simplicity, all correlation functions were fitted with a bi-exponential decay and the results are presented in Figure 2d, where we have plotted the correlation times, τ_f (fast mode) and τ_s (slow mode), of the two modes as a function of pH. At both extremes of pH, $\tau_f \approx \tau_s \approx 0.5$ ms, corresponding to a collective diffusion coefficient $D=(\tau q^2)^{-1} \approx 5 \cdot 10^{-12}$ m^{2}s^{-1}, where q is the scattering vector. This diffusion coefficient is in turn consistent with an apparent hydrodynamic radius $R_H \approx 40$ nm. This result implies that the peptide is aggregated also under these conditions, but the structures were not investigated further. In the gel regime, the correlation times increases and $\tau_f >> \tau_s$. A maximum is observed at pH≈8 with $\tau_s \approx 40$ ms and $\tau_f \approx 2$ ms, corresponding to the diffusion coefficients $D_s \approx 6\ 10^{-14}$ m^{2}s^{-1} and $D_f \approx 1\ 10^{-12}$ m^{2}s^{-1}, respectively. As will be shown below (Figure 4) the gel consist of rigid fibrils, with a cross section radius of $R \approx 2$ nm, which appear to be well dispersed, with no sign of lateral association or thicker bundles. Furthermore, the correlation functions decay to zero, demonstrating that the

system remains ergodic, also in the gel state. This indicates that the gel can be viewed as an entangled solution of thin rigid rods. Thus, a possible explanation for the two diffusion modes is that they correspond to diffusion perpendicular ($D_\perp$) and parallel ($D_\parallel$) to the fibril axis, respectively, with D_s=$D_\perp$ and D_f=$D_\parallel$, as was proposed recently[15] for another peptide system. There is also the possibility to observe the rotation mode. To discriminate between translation and rotation one would need to carry out measurements at several *q*-values, which is not possible with the present instrument. A more detailed analysis of the dynamics requires complementary experiments, and will be the topic of another study. $D_\perp$, as well as rotational diffusion, is strongly concentration dependent above the overlap concentration, while $D_\parallel$ is not.[15] Thus, it is possible to estimate a fibril length from $D_\parallel$.

In the limit of very large aspect ratios, the parallel diffusion coefficient for rigid rods is given by[16]

$$D_\parallel = \frac{k_B T}{2\pi\eta_0 L}\left(\ln\left(\frac{L}{R}\right) - 1.27\right) \quad (1)$$

where k_B is the Boltzmann's constant, T the absolute temperature, η_0 the solvent viscosity and R the rod cross section radius. Here, the peptide rods have a radius of R≈2 nm, as estimated from the *cryo*-TEM images (Figure 4) and the solvent viscosity, $\eta_0 \approx 10^{-3}$ Pa·s. Assuming that the fibrils behave as rigid rods, and that D_f=$D_\parallel \approx 1\ 10^{-12}$ m^2s^{-1}, we obtain a fibril length, L≈5 µm, which is a reasonable value. We hereby conclude here that the peptide forms very long fibrils at neutral pH, possibly ≈5 µm long, but more accurate and detailed light scattering experiments, including concentration dependence, are needed to confirm the assumed diffusion modes.

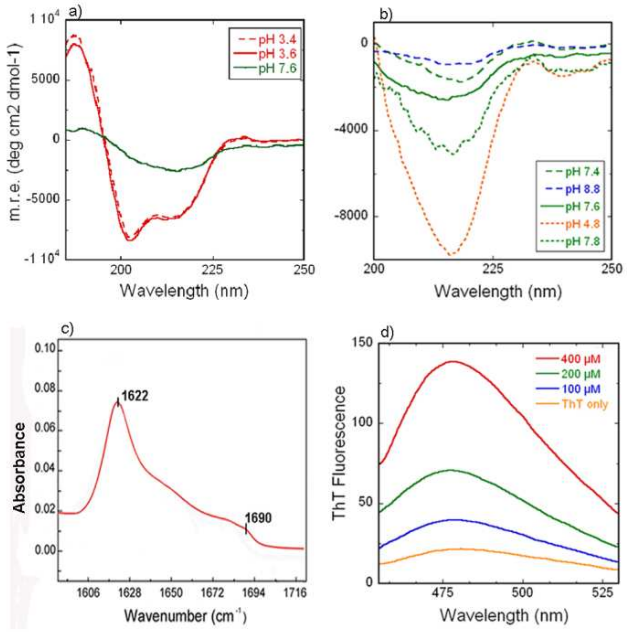

Figure 3. Secondary structure. Far-UV CD spectra of SgI:38-48 in water at (a) 2 mM, pH 7.6 (solid green), pH 3.6 (solid red) and 4 mM, pH 3.4 (red dashed line); (b) 1 mM (dotted line), 2 mM (solid line), and 4 mM (dashed line) at pH 4.8 (orange), 7.4-7.8 (green) and 8.8 (blue). (c) FTIR spectrum of 4 mM SgI:38-48 in water at pH 8. (d) Fluorescence emission spectra for 30 µM ThT in water (orange) and in water with 100 (blue), 200 (green) and 400 µM (red) SgI:38-48 at pH 7.

Secondary structure

FTIR and CD spectroscopy were used to study the secondary structure content of the SgI:38-48 peptide as a function of pH. At pH 3.6, samples of 2-4 mM peptide display water-like viscosity with no signs of gel formation (Figure 2). Under these conditions, the far-UV CD spectrum (Figure 3a) indicates a significant degree of secondary structure content, which was roughly estimated by spectral deconvolution using SELCON3,[17] to consist of 8% helix, 38% β-sheet, 22% turns and 32% random coil conformation. A 1 mM peptide sample at pH 4.8 remains fluid, but displays a CD spectrum with a minimum at 215 nm, which is typical for β-sheet (Figure 3b). At pH 7.6, a highly viscous gel is observed (Figure 2a) with reduced CD signal intensity, as might be expected due to light scattering by the gel. The CD spectrum, however, remains qualitatively the same within the pH range of gel formation (Figure 3b) implying that β-sheet structure dominates. The FTIR spectrum (Figure 3c) recorded for 4 mM peptide at pH 8.0 contains signals from amide carbonyl (C=O) stretches consistent with a mixture of β-sheet (1622 cm^{-1}) and random coil (1650 cm^{-1}). The small additional signal at 1690 cm^{-1} is further indicative of extended β-sheet structure. This particular combination of vibrational frequencies at around 1620 and 1690 cm^{-1} has been seen for other sheet-forming hydrogels, which has been suggested to arise from of an antiparallel β-sheet.[8] Calculations based on empirical residue-residue potentials[18] suggest a slight preference for an anti-parallel over an parallel arrangement (see SI, Figure SI-6). Electrostatic repulsion between end charges may further disfavor the parallel orientation, suggesting that an antiparallel organization might be the preferred mode of packing for SgI:38-48, although the orientation in-sheet and between sheets need not be the same.[19]

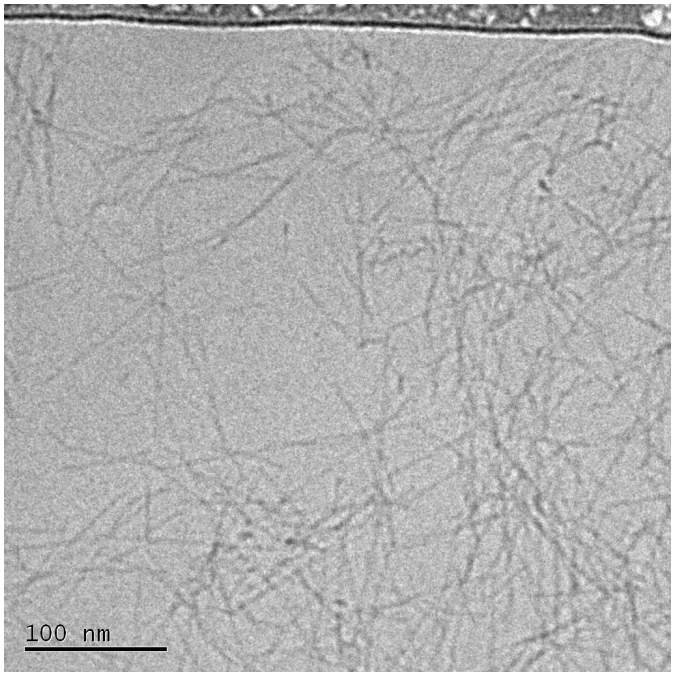

Figure 4. Gel morpholgy. *Cryo*-TEM image of a rapidly frozen gel formed from 4 mM SgI:38-48 peptide in water at pH 8.4.

Hydrogel morphology and fibril formation

The morphology of the gel (rapidly frozen) was studied with *cryo*-TEM. The data reveal a loose network of elongated (> 1 µm) fibrils

of ca. 4 nm diameter (Figure 4). Thioflavin T, ThT, binds to β-sheet aggregates with a resulting increase in fluorescence quantum yield and may be used to monitor fibril formation.[20] Due to the high sensitivity of this method, peptide concentrations at the limit for fibril formation and higher can be investigated. Here, we compare the ThT fluorescence spectrum in the absence and presence of 0.1-0.4 mM SgI:38-48 at pH 7.0. The enhanced quantum yield (Figure 3d) indicates that fibrillar aggregates are formed and that the amount of aggregates is roughly proportional to the peptide concentration. Consistent with the dynamic light scattering experiments discussed above (Figure 2c,d) the data indicate that 0.1 mM (0.01 % w/v) is well above the critical aggregation concentration. In Figure 5 are shown typical aggregation curves for 264 μM peptide solutions, with ThT fluorescence intensity recorded as a function of time starting from a monomeric sample isolated by size exclusion chromatography just prior to initiating the experiment. Sigmoidal curves are observed with a lag phase, a more rapid growth phase and a final plateau at which the signal stays relatively constant. The time-dependence of fibril formation is thus similar to that observed for several amyloid-forming proteins and peptides, indicating that gel formation of SgI:38-48 peptide is a nucleated reaction.[21]

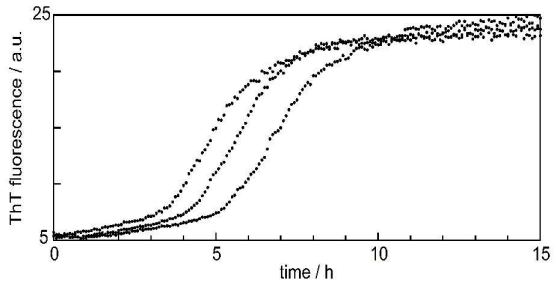

Figure 5. Fibril formation kinetics. Fibril formation as a function of time monitored by ThT fluorescence for three replicates of initially monomeric SgI:38-48 peptide at 264 μM in water, pH 8.0, 37 °C.

Rheology

The rheological properties of the hydrogel were characterized using dynamic oscillatory shear experiments. Small amplitude dynamic tests provide information on the linear viscoelastic behavior of materials through the determination of the complex shear modulus.[22] After loading, the peptide samples were allowed to relax over a period of 3 hours before the oscillatory experiments were conducted. This allows for stress relaxation and recovery of any reversible microstructural deformation during the loading process. At first, a shear strain amplitude sweep was performed, at ω = 10 rad/s, to determine the linear viscoelastic range. The results are presented in Figure 6a. The linear regime, where G' and G'' remain constant, stretches approximately up to γ =1 %, γ being the strain amplitude. Here, G' is approximately an order of magnitude larger than G'', thus the material behaves as an elastic gel.[15] At larger strain, the gel structure is deformed and G' decreases dramatically. Eventually $G'<G''$ and the material flows. Upon entering the nonlinear regime with increasing strain, the shear stress, σ, goes through a maximum. This marks the viscoplastic yield point associated with the rapid decrease in G' with strain. The characteristic yield values are σ_y=13.6 Pa and γ_y=4.8%. Moreover, the onset of complete fluidization from solid-like to liquid-like response can be determine at $G'= G''$ with respective stress and strain values as σ_f=5.4 Pa and γ_f=11.4%; γ_y and γ_f are indicated in Figure 6.

A non-destructive frequency sweep experiment, within the linear viscoelastic range was performed over a large angular frequency interval $5\cdot10^{-3}$ rad/s ≤ ω ≤ $2\cdot10^{2}$ rad/s. The strain amplitude was chosen to 0.2 %. The variations of G' and G'' with the oscillation angular frequency, ω, are presented in Figure 6b. The data are similar to those reported by Yucel *et al.* for a β-hairpin peptide,[23] as well as for other hydrogel forming peptides reviewed by Zuidema *et al.*[5]

As can be seen, the material responds as an elastic solid with $G' >> G''$ over the whole frequency range and additionally at the lowest frequency, $5\cdot10^{-3}$ rad/s. This means a characteristic stress relaxation time, τ >200 s. For a transient network of overlapping rigid rods, the stress is relaxed by the rods renewing their neighboring contacts by diffusing a distance parallel to the rod axis, essentially equal to their contour length, L. We thus have

$$\tau \approx \frac{L^2}{D_{\parallel}} \qquad (2)$$

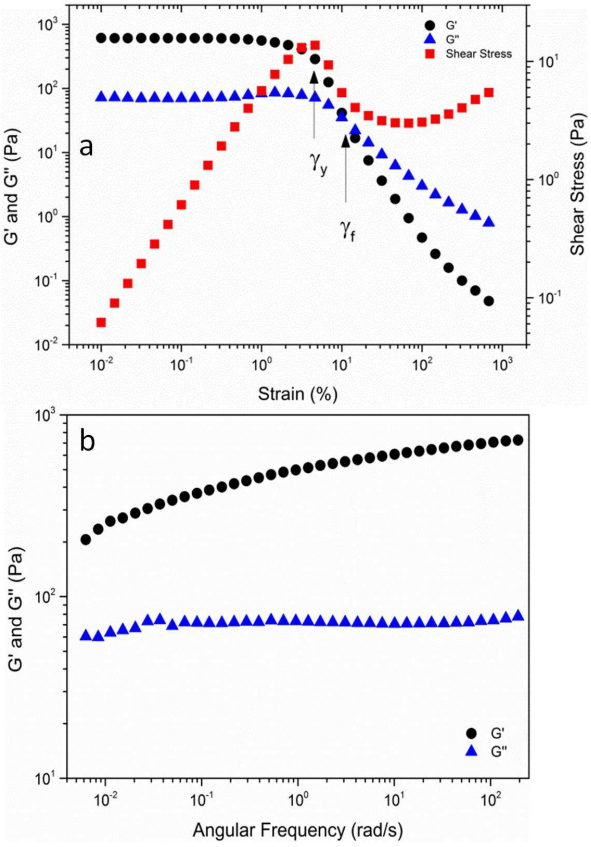

Figure 6. Rheology. Linear viscoelastic behavior of a gel sample of 0.5 mg/ml. **a)** Dynamic strain sweep test to determine the linear viscoelastic range and to characterize yielding. The yield point is determined from the maximum of the stress curve. The vertical arrows indicate the yield strain, γ_y, and point of complete fluidization, γ_f. **b)** Frequency sweep experiment performed in linear viscoelastic regime.

With these values and T=298 K, we obtain, with Eq. (1) and (2), a value of τ >200 s, which is consistent with a peptide fibril length L> 2 μm. This value is consistent with the DLS results, from which L≈5 μm was obtained. The very large aspect ratio (L/R >10^3) is also consistent with the fact that the present system shows a gel-like behavior already at a very low peptide concentration. The present concentration, 0.5 mg/ml is clearly in the semi-dilute regime, significantly above the overlap concentration. The overlap concentration (volume fraction), ϕ^*, can be estimated from

$$\phi^* \approx \frac{6R^2}{L^2} \quad (3)$$

For R=2 nm and L≈5 µm, Eq. (4) predicts ϕ^*≈10^{-6} which is more than two orders of magnitude lower than the concentration used here.

Our data represent the first rheological characterization of SgI:38-48 for which an elastic gel is formed at very low peptide concentration. Further characterization, including temperature and concentration dependence of dynamics and rheological properties is necessary to fully understand its behavior and to be able to further compare to other peptide systems.[6b] In particular, it would be interesting to evaluate whether the observed rheological behavior arises from the system being near dynamic arrest or glass formation,[24] and to understand the competition between this isotropic state and the nematic phase predicted for hard and charged rods.[25] We note that the gel is relatively stiff (G'>100 Pa) considering the low peptide concentration, indicating that the fibrils have a large bending rigidity. A possible reason for a high rigidity could be that the fibrils have an ordered structure, similar to fibrils of A_8K and $A_{10}K$ where the molecules are packed with crystalline order.[15] We further expect that the elastic modulus can be tuned by simply varying the peptide concentration. Theory predicts[26] $G' \sim \phi^2$, and the peptide concentration used here was rather low (0.5 mg/ml). Thus, it should be possible to vary the modulus over several orders of magnitude and to reach moduli in the MPa regime.

Cytotoxicity

The cytotoxicity of the peptide up to a concentration of 1 mM was studied in leukemia cells using the MTT assay. No cytotoxicity was observed (Figure 7).

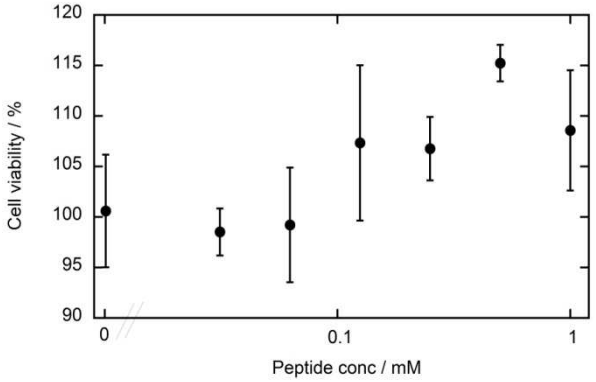

Figure 7. Cell viability as studied using the MTT assay for samples containing up to 1 mM (logarithmic scale) SgI:38-48 peptide at pH 7.0-7.4.

The spectroscopic and microscopic data (Figure 3 and 4) for GSFSIQYTYHV are consistent with a peptide that self-assembles into long fibrils of extended β-sheet, as commonly found for sequences of alternating hydrophobic and hydrophibic residues, a distinct feature of this peptide (Figure 1). The gel-like properties arise from a transient network formed by overlapping fibrils. At pH 3 the peptide net charge is between +1 and +2, with the N-terminus and His side chain positively charged, while the C-terminus might be partially negatively charged. Inter-peptide repulsion thus prevents gel formation at low pH. Upon pH neutralization, the N-terminus and His side-chain deprotonate. The peptide net charge changes towards zero, facilitating self-assembly and fibril formation. The optimal gel stability between pH 7 and 9 clearly correlates with the peptide's iso-electric point of 7.8. At pH 10 and beyond, the Tyr side chains ionize, the peptide becomes negatively charged and the critical aggregation concentration is expected to increase. Other amphiphilic peptides have similarly shown to assemble into β-sheet rich fibrils via back-bone hydrogen bonds in an orientation that optimizes the interactions between side-chains.[27] In these fibrils, hydrophobic side chains interact on one (dry) side of the sheet interface and hydrophilic on the other (wet) interface.[28]

Many types of peptide and protein based hydrogels exist, most of them produced synthetically or recombinantly.[1] Gels may be formed from repeating protein binding domains,[29] which self-assemble to generate oligomeric structures, such as coiled coils,[30] and other types of designed protein assemblies[31]. Co-block polymers, consisting of a hybrid of different types of polymers, such as polyethylene glycol (PEG) in combination with peptides,[32] or of a combination of two different types of peptides,[33] have also been explored for tailored properties. A variety of short, designed peptide sequences generate gels, including amphiphilic sequences[1g] and β-hairpin-forming peptides[1f]. Among naturally occurring proteins, gel systems based on gelatin and silk sequences have been studied extensively, but are still not fully understood due to their complexity. Proteins that provide a gel matrix also exist naturally, as in the entrapping and protection of spermatozoa by the proteins SgI and SgII. The gel properties of peptide segments of such proteins are of particular interest, providing sequence-based insights into the gel properties of these proteins. Using natural gel-forming proteins as a starting point offers a means to generate naturally derived sequences that are conceptually simple and potentially of low toxicity and immunogenicity, and therefore of great potential for biomaterials applications.

Experimental

Peptide synthesis and purification

The GSFSIQYTYHV peptide was synthesized using solid-phase methodology (Wang resin), employing a standard Fmoc-chemistry protocol, utilizing an Applied Biosystems 433A or a PS3 Protein Technologies Peptide Synthesizer. A 1:1 mixture of HBTU (*O*-Benzotriazole-*N,N,N',N'*-tetramethyl-uronium-hexafluoro-phosphate) and HOBt (*N*-hydroxybenzotriazole) was used in the activation of the free carboxylic acids at 4 to 10 molar equivalents. β-Branched amino acids and residues immediately following a β-branched residue were coupled twice. The cleavage of the peptide from the resin was achieved with trifluoroacetic acid (TFA)/thioanisole/1,2-ethanedithiol/anisole in a volume ratio of 9.0/0.5/0.3/0.2 for 2 h at room temperature. The solution was then concentrated with a stream of N_2 gas and the crude peptide precipitated with ice-cold diethyl ether, collected by filtration, dissolved in a mixture of water and acetonitrile and lyophilized. The crude peptide was purified by HPLC (Vydac C4) and the linear gradient of water, containing 0.1% TFA by volume (solvent A), and acetonitrile:water 9:1, containing 0.1% TFA (solvent B), with 1% increase in solvent B per min (Figure SI-3). The identity of the peptide was verified by matrix assisted laser desorption ionization mass spectrometry (MALDI-TOF MS; theoretical m/e 1301.6 experimental m/e 1301.6; Figure SI-4, and its purity by analytical HPLC (Figure SI-3b) adn NMR spectroscopy (Figure SI-5).

Hydrogel formation by visual inspection

Hydrogel formation of SgI:38-48 was visually examined as a function of pH (3.3-11.2), peptide concentration (1-4 mM), temperature (25 and 37 °C), NaCl concentration (0, 0.15 and 0.5 M), buffer concentration (0 or 50 mM Tris/HCl pH 8.5), co-solvent (0 or

5% v/v DMSO) or time (0-24 h). The peptide was dissolved in water, buffer or salt solution and pH adjusted using small (< 1µl) additions of NaOH and a thin pH electrode (3 mm diameter, Mettler Toledo) in clear polycarbonate tubes. The amount of NaOH required to reach each pH value was recorded resulting for example at pH 8.0 in a Na^+ concentration ca. 2 times the peptide concentration. After incubation for the designated time, gel formation was examined by slowly turning the tube and observing the fluidity vs. viscosity of the sample. The grade of viscosity was scored as follows: 0 - water like, 1 - slowly flowing, 2 - viscous with gel clumps along tube wall, 3 - highly viscous.

DLS

Dynamic light scattering was used to obtain measures of peptide aggregation as a function of pH using a DynaPro DLS plate reader II (Wyatt Technology Corp.). The laser wavelength was 830 nm and the scattering angle 158°, corresponding to a scattering vector q=0.0198 nm^{-1}. Lyophylized sgI:38-48 peptide was dissolved in water to 0.4 mM (0.5 mg/mL) and filtered through a size-exclusion filter (Vivaspin 15R hydrosart membrane with 30 kDa cutoff) to remove dust and possible aggregates. The pH was then adjusted by addition of small (sub µl) volumes of NaOH to 100 µl sample aliquots which were kept on ice prior to the measurements. Each sample was split in two and placed in two wells of a non-binding black 384-well plate with clear bottom (Corning) which was placed in the DLS reader at 25 C. Data for each sample were acquired for 3 sec. with 10 acquisitions and 10 cycles at 25°C**.** The auto-correlation function was recorded from 1 µs to 100 ms and its intensity normalised to occur between 1.0 and 0.0. The autocorrelation data at each pH were fitted both by a single exponential decay, and by a double exponential decay.

Aggregation kinetics by ThT fluorescence

Lyophylized SgI:38-48 peptide (1.5 mg, 1.15 umol) was dissolved in 6 M GuHCl, pH 3.5 (250 µL) and the monomer isolated by gel filtration with an eluent of 5 mM ammonium acetate buffer, pH 3.5, employing two 1x30 cm Superdex peptide columns connected in tandem. The monomer concentration of the collected fraction was determined to 264 µM based on the absorbance at 280 nm and using a molar absorptivity of 2,800 $M^{-1}cm^{-1}$ (calculated from the amino acid composition with two tyrosine residues). The pH of the monomer solution was raised to 8.0, and thioflavin T was added to a final concentration of 26 µM from a concentrated stock. Three identical 80 µl samples were placed in three wells of a non-binding 96-well plate (Corning 3881) and the fluorescence intensity recorded every 5 min through the bottom of the wells at 37 °C in a BMG Omega Plate reader using an excitation and an emission filter of 440 and 480 nm, respectively.

CD spectroscopy

Far-UV CD spectra were recorded between 250 and 185 nm for 1-4 mM samples in water in 0.1-0.2 mm quartz cuvettes at 25 ºC using a JASCO J-815 spectropolarimeter with the following settings: sensitivity standard, data integration time 8 s, scan rate 20 nm/min, number of accumulations 3.

FTIR spectroscopy

FT-IR spectra were acquired using a Bruker Optics, Inc. Vertex 70 FT-IR with OPUS software. Samples were mounted in a Harrick demountable liquid cell using CaF_2 salt plates and a 50 µm path length Teflon spacer. In a typical experiment, residual TFA was first exchanged for chloride by dissolving pure SgI:38-48 (2.6 mg) in 1 mL H_2O and adjusting the pH to 2.06 with dilute HCl. After lyophilization, the sample was twice dissolved in 400 µL D_2O, frozen and lyophilized. A spectrum was then obtained of a sample prepared in D_2O at 5 mg/mL (3.8 mM) with a background spectrum in D_2O subtracted.

cryo-TEM

A gel formed from 4 mM SgI:38-48 peptide at pH 8.4 was prepared as a thin liquid film, <300 nm thick, on lacey carbon filmed copper grids and plunged into liquid ethane at -180 °C. This leads to vitrified specimens, avoiding component segmentation and rearrangement, and water crystallization, thereby preserving original microstructures. The vitrified specimens were studied using an electron microscope (Philips CM120 BioTWIN Cryo) equipped with a post-column energy filter (Gatan GIF100). The acceleration voltage was 120 kV. The images were recorded digitally with a CCD camera under low electron dose conditions.

Rheology

Rheology measurements were carried out on an Anton Paar Physica MCR 301 instrument equipped with a cone-plate geometry, 50 mm diameter, 1º angle. The temperature was fixed at 25 °C and controlled by a Peltier system. To minimize evaporation, the measuring geometry was surrounded by a solvent trap containing water. Dynamic oscillatory shear experiments were performed. The small amplitude dynamic tests provided information on the linear viscoelastic behavior of materials through the determination of the complex shear modulus.[16] The linear viscoelastic regime was determined from a strain sweep test at ω=10 rad/s. Here strain was varied over five orders of magnitude, between 0.01 and 1000%.

Cytoxicity Studies

MTT (3-(4,5-dimethylthiazol-2-yl)-2,5-diphenyltetrazolium bromide) assay. The effect of SgI 38-48 on the viability of L1210 murine lymphocytic leukemia cells *in vitro* was assessed by an MTT assay. L1210 cells were donated by Dr. Jennifer Punt (Haverford College, PA). Cells were cultured in medium, RPMI-1640 (Gibco Invitrogen, USA) supplemented with 10% FBS (fetal bovine serum, HyClone Thermo Scientific, USA), 2.05 mM L-glutamine (Gibco Invitrogen, USA), 50 µg/mL Pen/Strep antibiotics (Gibco Invitrogen, USA), 1% NEAA (non-essential amino acids solution, Gibco Invitrogen, USA), and 1% Na-Pyruvate (Sigma-Aldrich, USA) in 5% CO_2 at 37 °C. Cells were seeded in 96-well plates at a density of 4×10^4 cells/well with fresh medium (90 µL). Peptide concentrations ranging from 30 – 1000 µM were added to each of the wells (10 µL aliquots, sterile water for controls) and incubated for 48 h. Subsequently, 25 µL of MTT solution (5 mg/mL MTT in H_2O; Sigma-Aldrich, USA) was added to each well and the plates were incubated at 37 °C for 2 h. Thereafter, 20% SDS/50% DMF (100 µL; both from Sigma-Aldrich, USA) was added to each well to solubilize the formazan crystals and the plates were incubated overnight. The absorbance was measured at λ = 570 nm with background subtraction at 492 nm employing a TECAN SpectraFluor Plus (MTX Lab Systems, USA). Cell viability was determined relative to untreated controls. Each sample point was performed in triplicate.

Conclusions

In this work, we have shown that a peptide derived from human SgI (residues 38-48, GSFSIQYTYHV) forms a pH-responsive hydrogel at low peptide concentration (1 mM = 0.1 % w/v) with characteristic viscoelastic properties. Upon neutralization, a clear gel forms through the spontaneous self-assembly of the peptide into µm long fibrillar aggregates composed of extended β-sheets. We detect no cytotoxicity up to 1 mM peptide concentration and being of human origin the peptide is not likely to elicit an immune response. In contrast to many other peptides, the SgI:38-48 peptide does not

precipitate around the iso-electric point, which in this case is close to neutral pH. A structural switch at neutral pH provides an ideal means for tuning its materials properties under physiologically relevant conditions. The SgI 38-48 peptide may therefore serve as a basis for future development of smart biomaterials suitable for applications in the biomedical field, including drug delivery and wound healing.

Acknowledgements

We thank Ulrich Weininger, Casey Londergan and Eric Holowka for fruitful discussions.. We are grateful for monetary support from the Swedish Research Council and its Linnaeus Centre Organizing Molecular Matter, OMM (SL, UO), the nanometer structure consortium at LU (SL), the Gyllenstierna Krapperup's Foundation (UO), and the Koshland Integrated Natural Science Center, Haverford College, US (JED, KSA). This work was also co-financed by the European Commission, European Social Fund, and the Region of Calabria (LG). The authors are solely responsible for this article, and the European Commission and the Region of Calabria are not responsible for any use that may be made of the information contained herein. We are indebted to Beatrice Ary and Shelby Lyons for the synthesis and HPLC purification of the peptide samples used for the ThT, rheology and MTT studies and for participating in investigations related to this work.

Notes and references

[a] Biochemistry and Structural Biology, Lund University, P O Box 124, SE-221 00 Lund, Sweden.
[b] Chemistry Department, Haverford College. 370 Lancaster Ave, Haverford, PA 19041, US.
[c] University of Pennsylvania, Biochemistry & Biophysics, PA 19041, US.
[d] Abramson Family Cancer Research Institute, Perelman School of Medicine at the University of Pennsylvania, Philadelphia, PA 19104, US.
[e] Physical Chemistry, Lund University, P O Box 124, SE-221 00 Lund, Sweden.
[f] Clinical Chemistry, Lund University, Skåne University Hospital, SE-205 02 Malmö, Sweden.

† Electronic Supplementary Information (ESI) available: Supplementary text and 6 supplementary Figures. See DOI: 10.1039/b000000x/.

1. (a) C. Yan, D. J. Pochan, *Chem. Soc. Rev.* 2010, **39**, 3528-3540; (b) J. Zhu, R. E. Marchant, *Expert Rev. Med. Devices* 2011, **8,** 607-626; (c) J. Kopeček, J.Yang, *Angew. Chem. Int. Ed. Engl.*2012, **51**, 7396-7417; (d) J. Y. Sun, X. Zhao, W. R. K. Illeperuma, O. Chaudhuri, K. H. Oh, D. J. Mooney, J. J. Vlassak, Z. Suo. *Nature* 2012, **489**, 133-136; (e) M. N. V. R. Kumar, *React. Func. Polym.* 2000, **46**, 1-27, (f) K. Rajagopal, J. P. Schneider, *Curr. Opin. Struct. Biol.* 2004, **14**, 480-486; (g) H. Zhang, X. Zhao, H. Luo, *J. Nanotech. Eng. Med.* 2010, **1**, 011007.
2. A. S. Hoffman *Adv. Drug Delivery Rev.* 2012, **64**, 18-23.
3. P. B. Malafaya, G. A. Silva, R. L. Reis *Adv. Drug Delivery Rev. 2007,* **59**, 207-233.
4. (a) K. Y. Lee, D. J. Mooney *Chem. Rev.* 2001, **110**, 1869-1879; (b) I. Gibas, H. Janik, *Chemistry and Chemical Technology* 2010, **4**, 297-304.
5. J. M. Zuidema, C. J. Rivet, R. J. Gilbert, F. A. Morrison *J. Biomed. Mater. Res. Part B: Appl. Biomater.* 2014, **102**, 1063-1073.
6. (a) A. Dasgupta, J. H. Mondal, D. Das *RSC Advances* 2013, **3**, 9117-9149; (b) L. Dooling, D. A. Tirrell (2013) Peptide and Protein Hydrogels In: Polymeric and self assembled hydrogels: from fundamental understanding to applications. Monographs in supramolecular chemistry. No.11. Royal Society of Chemistry , Cambridge, UK, pp. 93-124 (c) N Stephanopoulos, J. H. Ortony, S. I. Stupp *Acta Mater.* 2013, **61**, 912–930; (d) J. Kopeček, J. Yang *Acta Biomater.* 2009, **5**, 805–816; (e) S. Boothroyd, A. F. Miller, A. Saiani. Faradat Trans. 2013, **166**, 195-207.
7. E. Holowka, S. Bhatia Drug Delivery: Material Design & Clinical Perspective, Springer (in press).
8. N. R. Lee, C. J. Bowerman, B. L. Nilsson *Biomacromolecules* 2013, **14**, 3267-3277.
9. Y. Qiu, K. Park *Adv. Drug Delivery Rev.* 2012, **64**, 49-60.
10. (a) L. Goldschmidt L, P. K. Teng, R. Riek R, D. Eisenberg *Proc. Natl. Acad. Sci. U. S. A.* 2010, **107**, 3487-3492 (b) A. W. Fitzpatrick, T. P. Knowles, C. A. Waudby, M. Vendruscolo, C. M. Dobson *PLoS Comput. Biol.* 2011, **7**, e1002169.
11. (a) A. Nagai, Y. Nagai, H. Qu, S. Zhang. J. Nanosci. Nanotechnol. 2007, 7, 2246-2252. (b) S. Zhang *Acc. Chem. Res.* 2012, **45**, 2142-2150.
12. L. Adler-Abramovich, D. Aronov, P. Beker, M. Yevnin, S. Stempler, L. Buzhansky, G. Rosenman, E. Gazit *Nature Nanotech.* 2009 **4**, 849 – 854.
13. (a) T. Nonoyama, H. Ogasawara, M. Tanaka, M. Higuchi, T. Kinoshita *Soft Matter* 2012, 8, 11531-11536; (b) H. Wang, Z. Yang *Nanoscale* 2012, **4**, 5259-5267; (c) G.-J. Wei, M. Yao, Y.-S. Wang, D.-Y. Wan, P.-Z. Lei, J. Wen. H.-W. Lei, D.-M. Dong *Int. J. Nanomedicine* 2013, **8**, 3217-3225.
14. (a) A.Lundwall, A. Bjartell, A. Y. Olsson, J. Malm, *J. Mol. Hum. Reprod.* 2002, **8,** 805-810; (b) V.L. Bonilha, M. E. Rayborn, K. G. Shadrach, Y. Li, Å. Lundwall, J. Malm, J. G. Hollyfield. *Exp. Eye Res.* 2006, **283**, 120-127; (c) M. Jonsson, S. Linse, B. Frohm, Å. Lundwall, J. Malm. *Biochem. J.* 2005, **387**, 477-453; (d) J. Malm, M. Jonsson, M, B. Frohm, S. Linse, *FEBS J.* 2007, **274,** 4503-4510; (e) M. Jonsson, B. Frohm, J. Malm, *J. Androl.* 2010, **31,** 560-565; (f) K.P. Tremellen, D. Valbuera, J. Landeras, A. Ballesteros, J. Martinez, S. Mendoza, R. J. Norman, S. A. Robertson, C. Simón. *Hum. Reprod.* 2000, **15**, 2653-2658; (g) V. N. Uversky, *J Biomed. Biotechnol.* 2010, 568068; (h) Malm, J.; Hellman, J.; Hogg, P.; Lilja, H. *Prostate* 2000, **45**, 132-139.
15. C. C. Cenker, S Bucak, U. Olsson *Langmuir*,2014, **30**, 10072-10079.
16. (a) S. Broersma *J. Chem. Phys.* 1960, **32**, 1632-1635; (b) K. M. Zero, R. Pecora *Macromolecules* 1982, **15**, 87-93.
17. N. Sreerama, S. Y. Venyaminov, R. W. Woody. *Anal Biochem.* 2000, **287**, 243-251.
18. O. Keskin, I. Bahar, A. Y. Badretdinov, O. B. Ptitsyn, R. L. Jernigan. *Protein Sci*. 1998, **7**, 2578-2586.
19. D. Eisenberg, M. Jucker. *Cell* 2012, **148**, 1188-1203.
20. L. S. Wolfe, M. F. Calabrese, A. Nath, D. V. Blaho, A. D. Miranker, Y. Xiong. *Proc. Natl. Acad. Sci. U.S.A.* 2010, **107**, 16863-1686820.
21. J.T. Jarrett, P.T. Lansbury, *Cell* 1993, **73**, 1055-1058.
22. (a) J. D. Ferry Viscoelastic Properties of Polymers 3rd ed., Wiley, New York, 1980; (b) R. G. Larson, The Structure and Rheology of Complex Fluids, Oxford University Press, New York, 1999.
23. T. Yucel, C. M. Micklitsch, J. P. Schneider, D. J. Pochan *Macromolecules* 2008, **41**, 5763-5772.
24. (a) K. Kang, J. K. G. Dhont *Phys Rev Lett* , 2013, **110**, 015901; (b) M. J. Solomon, P. Spicer, 2010, **6**, 1391–1400.
25. (a) L. Onsager, *Annal. N. Y. Acad. Sci.* 1949, **51**, 627-659; (b) A. Stroobants, H. N. W. Lekkerkerker, T. Odijk, *Macromolecules*, 1986, **19**, 2232-2238.
26 J. L. Jones, C. M. Marques *J. Phys.* 1990, 51, 1113-1127.
27. (a) A. Brack, L.E. Orgel, *Nature* 1975, **256**, 383-387; (b) C. K. Smith, L. Regan, *Science* 1995, **270**, 980-982; (c) S. Zhang, T. C. Holmes, C. M. DiPersio, R. O. Hynes, X. Su, A. Rich. *Biomaterials* 1995, **16,** 1385-1393; (d) M. W. West, W. Wang, J. Patterson, J. D. Mancias, J. R. Beasley, M. H. Hecht. *Proc. Natl. Acad. Sci. U.S.A.* 1999, **96,** 11211-11216.; (e). Goldschmidt, P. K. Teng, R. Riek, D. Eisenberg, *Proc. Natl. Acad. Sci. U.S.A.* 2010, **107**, 3487-3492.
28. R. Nelson, M. R. Sawaya, M. M. Balbirnie, A. Ø. Madsen , C. Riekel, R. Grothe, D. Eisenberg. Nature 2005, 435, 773-778.
29. T. Z. Grove, C. O. Osuji, J. D. Forster, E. R. Dufresne, L. Regan L 2010 *J. Am. Chem. Soc.* **132**, 14024–14026.
30 E. F. Banwell, E. S. Abelardo, D. J. Adams, M. A. Birchall, A. Corrigan, A. M. Donald, M. Kirkland, L. C. Serpell, M. F. Butler, D. N. Wolfsson *Nat. Mater.* 2009, **8**, 596-600.
31. X. Zhang, X. Chu, L. Wang, H. Wang, G. Liang, et al. *Angew. Chem.,-Int. Ed*. 2012 **51**: 4388–4392.
32. H. M. König, A. F. M. Kilbinger *Angew. Chem. Int. Ed*. 2007, **46**:2–9.
33. W. Mulyasasmita, J. S. Lee, S. C. Heilshorn *Biomacromolecules* 2011,. **12** 3406–3411.